J Mater Sci (2008) 43:759–765
DOI 10.1007/s10853-007-2180-y

Microstructure and mechanical properties of fluorcanasite glass-ceramics for biomedical applications

Naruporn Kanchanarat · Sanchita Bandyopadhyay-Ghosh · Ian M. Reaney · Ian M. Brook · Paul V. Hatton

Received: 7 March 2007 / Accepted: 21 September 2007 / Published online: 31 October 2007

Abstract Four fluorcanasite glass-ceramics were fabricated by controlled heat-treatment of as-cast Glasses A–D. These compositions have been reported previously but essentially, Glass A had the stoichiometric composition ($Ca_5Na_4K_2Si_{12}O_{30}F_4$) and Glasses B–D were modified by reducing the Na_2O concentration (B), adding excess CaO (C) and P_2O_5 (D). The latter two compositions have been shown to have promising bioactive response in cell culture and simulated body fluid experiments. Devitrification of the stoichiometric composition resulted in poor mechanical properties with crumbling often observed on machining. As a result, no mechanical data could be obtained. In all modified compositions, heat-treatment between 780 °C and 900 °C resulted in measurable indentation fracture toughness (IFT) and biaxial flexural strength (BFS). IFT was optimised in Glass C at 800 °C (2.53 ± 0.02 MPa $m^{½}$), but the biaxial flexural strength (BFS) was low, 167 ± 17 MPa, compared to other compositions. For heat- treated Glass D optimum mechanical properties were obtained at 800 °C with BFS and IFT, 249 ± 23 MPa and 1.95 ± 0.01 MPa $m^{½}$, respectively. The relationship between the mechanical properties and microstructure is discussed.

N. Kanchanarat · S. Bandyopadhyay-Ghosh (✉) · I. M. Reaney
Department of Engineering Materials, University of Sheffield, Sir Robert Hadfield Building, Mappin Street, Sheffield S1 3JD, UK
e-mail: bg_sanchita@yahoo.co.uk

I. M. Brook · P. V. Hatton
Centre for Biomaterials and Tissue Engineering, School of Clinical Dentistry, University of Sheffield, Claremont Crescent, Sheffield S10 2TA, UK

Introduction

Many bioceramics, bioglasses and bioglass-ceramics have been investigated to improve their biocompatibility, osteoconductivity (bioactivity) and mechanical properties. Hydroxyapatite (HA) and Bioglass® show good biocompatibility and osteoconductivity, and are widely used as coatings or bone substitutes [1–3]. Their mechanical properties, however, make them unsuitable for fabrication of medical devices for load-bearing applications. In comparison, apatite–wollastonite (A–W) glass-ceramics introduced by Kokubo et al. [4] are bioactive and have excellent mechanical properties with a fracture toughness (FT) of 2–2.5 MPa $m^{½}$ and biaxial flexural strength (BFS) of 200 MPa. This makes them suitable for load bearing applications, and they have enjoyed clinical use in Japan as replacement vertebrae. The key limitation of A–W is that the strengthening phase, wollastonite, undergoes surface rather than bulk nucleation [4]. It may, therefore, only be processed via a sintered-powder route. Ideally, for clinical use, it is desirable to cast a glass (followed by controlled crystallisation) to form a custom prosthesis via the lost wax technique. Such a process requires that the glass has a low viscosity and volume nucleates the strengthening phase upon heat-treatment in order to optimise mechanical properties.

Chain silicate glass-ceramics such as enstatite, K-fluorrichterite and fluorcanasite glass-ceramics were reported to bulk nucleate and have good mechanical properties (BFS $>$ 300 MPa and FT $\sim$ 5 MPa $m^{1/2}$) [5, 6]. Unfortunately, early published fluorcanasite compositions showed poor in vivo biocompatibility and no osteoconductive properties [7]. More recently, there have been attempts to improve the biocompatibility and osteoconductive potential of fluorcanasite glass-ceramics by Miller et al. [8–11]. They reduced the Na_2O concentration, increased the CaO

content, and added P_2O_5 in several different glass series. In vitro biocompatibility studies in simulated body fluid (SBF) and using cell culture were subsequently reported by Miller et al. [10] and Bandyopadhyay-Ghosh et al. [12, 13] respectively. Kanchanarat et al. [14] investigated the early stages of nucleation and growth in the fluorcanasite compositions developed by Miller et al. [8–11] using transmission electron microscopy (TEM), which followed on from earlier detailed X-ray diffraction (XRD) work. No detailed studies of mechanical properties have been published, and there has been no attempt to relate the microstructure to the measured indentation fracture toughness (IFT) and biaxial flexural strength (BFS) values. The aim of this study was, therefore, to investigate the relationship between phase evolution, microstructure and mechanical properties of modified fluorcanasite glass-ceramics.

Experimental procedures

Glass preparation

Glass batches were prepared by mixing appropriate amount of silica (Loch Aline Sand 99.5%) $CaHPO_4$, Na_2CO_3, K_2CO_3 (Standard Laboratory Grade Chemicals, Fisher Scientific Ltd., UK) and CaF_2 (Aldrich Chemical Company, USA). Glass compositions (Table 1) were melted on the basis of procedures described by Miller et al. [8–11]. Batches were melted in an uncovered platinum-rhodium (2%) crucible at 1,450 °C for 3 h and stirred for the final 2 h to achieve homogeneity with the platinum stirrer rotating at 60 rpm. The glass melting time was optimised following [8–11] to reduce fluorine losses. The qualitative EDS of the glass matrix indicated that they contained elements (Ca, Si, K, Na, F) in agreement with the batch composition. Glasses were cast as a block onto a heated steel plate and annealed in a muffle furnace at 460 °C for 1 h to reduce the internal stress in the glasses followed by cooling to room temperature at 1 °C/min.

Heat-treatment

Samples were cut into pieces (~10 mm × 10 mm × 10 mm) and placed in an alumina tray and in a Lenton tube furnace (Lenton Ltd., Hope Valley, UK). A two-stage heat-treatment schedule was performed, in which glasses were heated to nucleating temperature of 550 °C by the heating rate of 5 °C/min, held for 2 h, and then ramped up to various crystal growth temperatures (e.g. 780 °C). The heating rate was 5 °C/min, and samples were held for 2 h followed by a furnace cool at 5 °C/min. to room temperature. Subsequent to heat-treatment, samples are referred to as glass-ceramic (GC) A–D.

Table 1 Glass compositions (mol%)

Oxide	SiO_2	CaO	CaF_2	K_2O	Na_2O	P_2O_5
Glass A Stoichiometric	60.0	15.0	10.0	5.0	10.0	0.0
Glass B Reduced Na_2O	63.5	15.9	10.6	5.3	4.8	0.0
Glass C Increased CaO	61.6	19.2	10.3	5.1	3.8	0.0
Glass D 2% P_2O_5	62.7	17.8	8.4	5.2	3.9	2.1

Scanning electron microscopy

A JEOL 6400 (JEOL Ltd, Tokyo, Japan) scanning electron microscope (SEM) was used to examine the fracture surfaces of fluorcanasite glass-ceramic materials after two stage heat-treatment (520 °C/2 h and 780 °C/2 h). The samples were mounted on aluminium stubs using silver paint, followed by gold coating using an Emscope SC500A sputter coating unit.

Transmission electron microscopy

Samples for transmission electron microscopy (TEM) were first cut from the cerammed body, mounted onto a metal stub using a thermosensitive resin and ground to <30 μm using a Gatan 600 polishing unit. A Cu support ring (3.05 mm, 1,000 μm hole) was then glued onto the ground sample, which was subsequently removed from the stub. Excess material was chipped away from the exterior of the support ring using a scalpel. Further thinning to a thickness of <200 nm was carried out using Gatan Dual Ion Beam Mill Model 600 DP and 600 TMP (Gatan Inc., Pleasanton, USA). Samples were thinned at an angle of 11–15°, at ~6 kV with combined gun current of 0.6 mA. After milling the specimens were carbon coated and analysed using Philips EM 420 TEM (Eindhoven, Holland) operating at 120 kV, equipped with an energy dispersive (EDS) X-ray detector and Link EDS hardware/software.

Indentation fracture toughness (IFT)

Glass specimens (40 mm × 30 mm × 40 mm) initially cut from the glass block with a diamond saw blade machine (Acutum 5, Struers, Ltd., Copenhagen, Denmark) to create parallel faces. After heat-treatment, they were polished down to 1 μm using SiC paper and ultimately with diamond paste. Indentations were obtained using Vickers hardness testing machine (Vicker-Armstrong, Ltd., Crayford, UK) for load higher than 1 kg (2.5, 5, 7.5, 12.5 and 15 kg) and a Vickers micro-hardness testing machine (Model M400, Leco

Corporation, St. Joseph, MO) for load lower than 1 kg (100, 200, 300, 500 and 1 kg). The used loads were restricted to a range, over which the indentation patterns remained well defined; at the lower end by the minimum requirement $c \geq 2a$, where c is the radial crack length and a is the indentation half-diagonal length, at the upper end by chipping or by the limitation of specimen thickness. For each load, at least 20–25 indentations were made, and at least 10–15 readings were taken using an optical microscopy Polyvar MET, Reichert-Jung equipped with a digital camera and computer (KS 400 software, Imaging Associations, Ltd., Thames, UK). Fracture toughness was calculated using the relations $K_{Ic} = 0.0824\ P/C^{3/2}$, where K_{Ic} is indentation fracture toughness (IFT), P is the indentation load and C is the radial crack size. To evaluate the crack types (median/radial or palmqvist), the samples were polished after indentation [15, 16] and examined using either transmission or reflection optical microscopy. Both as-cast glass and heat-treated samples exhibited indentation, in which the cracks were of the median/radian type.

Biaxial flexural strength

Glasses for each series were core drilled from the as-cast glass plates to obtain at least 10 disks (12 mm × 2 mm). After two stage heat-treatment, they were ground, and polished down to 1 μm using SiC paper and diamond paste. A ball on ring test-jig equipped with a universal testing machine (Model 2000R, Lloyds Instruments, Ltd., Fareham, Hampshire, UK) with a ring support of 9 mm at a cross-head speed of 1 mm/min. was performed on the samples. A sheet of paper was placed between the samples and support ring to eliminate any beyond flatness and reduce friction [17]. Each disk was marked the centre as the correct place of the loading ball before testing. The maximum stress, δ_{max} at the centre was calculated applying the following equation [18].

$$\sigma_{max} = \frac{3(1+v)P}{4\pi t^2}\left[1 + 2\ln\frac{a}{b} + \frac{(1-v)}{(1+v)}\left\{1 - \frac{b^2}{2a^2}\right\}\frac{a^2}{R^2}\right]$$

where P is load, t is disk thickness, a is radius of the circle of the support ring, b is radius of the region of uniform loading at the centre $b = t/3$, R is radius of the disk sample and v is Poisson's ratio, $v = 0.25$.

Results and discussion

Summary of the phase evolution

The phase evolution of Glasses A–D has been presented extensively by Miller et al. [8–11] and additionally Kanchanarat et al. [14] have studied the early stages of crystallisation. For a detailed discussion of the phase evolution, the reader is referred to these texts, but to facilitate a more complete understanding of the relation between phase evolution, microstructure and mechanical properties, the data is summarised in the following section.

Glass A is the stoichiometric composition, which upon heat-treatment homogeneously nucleates frankamenite, $K_3Na_3Ca_5(Si_{12}O_{30})F_4.H_2O$, a chain silicate similar in composition and structure to fluorcanasite, $Ca_5Na_4K_2Si_{12}O_{30}F_4$, without the presence of a nucleating phase. Frankamenite was shown by EDS to have the same composition as the parent glass and was the dominant phase at high temperature (>800 °C). Glass B forms CaF_2 crystals at low temperature (~600 °C), which act as nucleating sites for the formation of fluorcanasite (~750 °C). Gradually, at higher temperatures (>750 °C), the phase assemblage contains a mixture of frankamenite and fluorcanasite. For Glass C, CaF_2 crystals are observed at low temperatures (~550 °C), which act as nucleating sites for a xonotlite phase (~750 °C), which is replaced at higher temperatures (>750 °C) by fluorcanasite and frankamenite. Glass D is opalescent on casting, containing a mixture of CaF_2 and fluorapatite crystals. At ~700 °C, all crystals (both fluorapatite and CaF_2) are observed to act as nucleating sites for the chain silicate phase and at higher temperatures (>750 °C), fluorcanasite and frankamenite dominate.

Microstructure

Figure 1 shows the SEM micrograph of fracture surfaces of GCA-D780. In general, all SEM images showed fracture surfaces that consist of interlocking lath-like crystals. Higher growth temperatures showed qualitative similar fracture surfaces for all glass-ceramics. The microstructure generally consisted of interlocking lath-like crystals similar to those reported by Beall [5]. GCA780 however, was composed of laths considerably larger (>100 μm) than those observed in GCB-D780. The laths are difficult to be resolved in GCB780, and GCC780 and are <30 μm in GCD780. The large laths in GCA are responsible for its poor mechanical properties and the associated crumbling during grinding prohibited further investigation of the microstructure by TEM. It is evident however, that the major affect of all the compositional modifications is to reduce the crystallite size. Miller et al. [8–11] attributed the reduction in crystallite size for competition during growth between the frankamenite and fluorcanasite phases. The large laths in GCA arise due to the glass and crystal phase having the same composition. This results in unrestricted growth of frankamenite since only rearrangement of the glass structure is required ahead of the

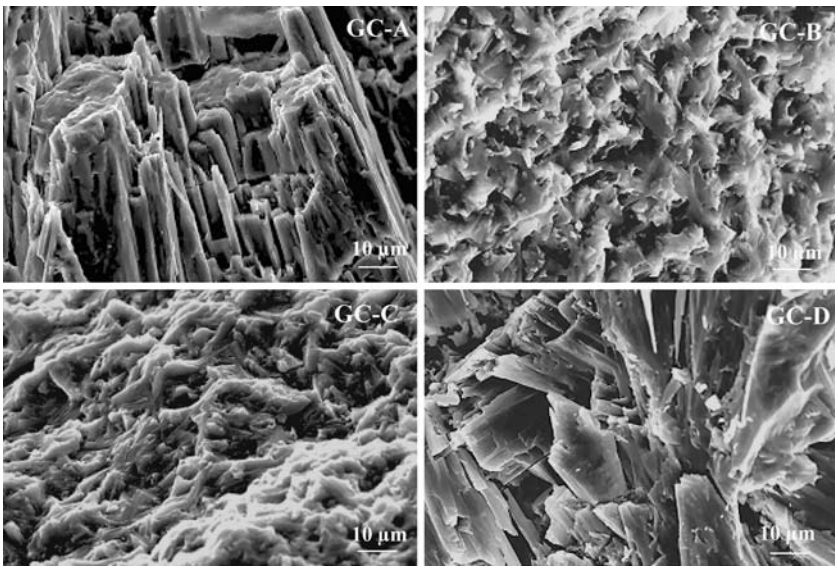

Fig. 1 SEM images of fracture surfaces of Glass-Ceramics A–D (GCA–GCD)

crystallisation front rather than diffusion to and from the crystal/glass interface.

The fact that microstructure could influence mechanical properties in a major way; led to the detail investigation of the crystal microstructure using TEM. With TEM result, the mean crystal length and width as well as the aspect ratio were obtained in a superior fashion compared to SEM images.

Figure 2a and b are bright field (BF) TEM images showing the microstructures of GCB800 and GCB900. At 800 °C, laths ($\sim 20 \times 0.15$ μm) are present, which according to XRD are fluorcanasite and frankamenite. At 900 °C, a qualitatively similar microstructure is observed, but the laths are coarser ($\sim 30 \times 0.2$ μm). In addition, the small voids (arrowed) observed at 800 °C are absent at 900 °C. The origin of the voids is unclear, but they may be the sites of the original CaF_2 crystals, which react with the residual glass during growth to form fluorcanasite. EDS from the laths (Fig. 2c) indicated that they contained Ca, Si, K and Na, but there was no reproducible quantitative difference between the spectra from the laths within the same sample and in samples heat-treated at different temperatures.

Figure 3a, b and c are BF TEM images of GCC800 and 900. At 800 °C, TEM images revealed lath shaped ($\sim 1 \times 0.05$ μm) crystals in addition to a large volume of residual glass, rarely observed in GCB800. According to XRD, the laths are a mixture of fluorcanasite and frankamenite at 800 °C, although at 700 °C, xonotlite is the first chain silicate phase to nucleate. At 900 °C, the residual glass phase was absent and laths had coarsened ($\sim 20 \times 0.2$ μm). EDS did not reveal any reproducible quantitative differences between laths in GCC800 and GCC900 and spectra were similar to that shown in Fig. 2c.

Figure 4a, b and c shows the BF TEM images of Glass D, heat-treated 2 h at 800 °C and 900 °C. At 800 °C, laths (20×0.1 μm) of frankamenite and fluorcanasite dominate the (~ 50 nm) microstructure, but intragranular spherulites may be observed, which are P rich with respect to laths. According to XRD [8–11], fluorapatite is present at this temperature in agreement with Wolcott [19]. The microstructure remains qualitatively similar at 900 °C, but the frankamenite and fluorcanasite laths (50×0.2 μm) and spherulites (0.2 μm) have coarsened.

Mechanical properties

Glass A is excluded from the investigation since this composition crumbles on grinding when heated at >700 °C.

Indentation fracture toughness (IFT)

Figure 5 shows the IFT values of Glass B, C and D as-cast and heat-treated at different temperatures. The as-cast glasses gave the lowest fracture toughness, <0.7 MPa $m^{1/2}$, but all cerammed materials exhibited values >1.5 MPa $m^{1/2}$.

The highest IFT for all samples was obtained at 800 °C with Glass B, C and D, 2.25 ± 0.01 2.53 ± 0.02 and 1.95 ± 0.01 MPa $m^{1/2}$, respectively, which suggests that this heat-treatment temperature is close to the optimum, possibly due to the finer microstructure, as illustrated in Fig. 2a, b and c. Beall et al. [20] suggested that the source of the high fracture toughness in chain silicate glass-ceramics is related to microcrack toughening from the internal stresses that arise from the thermal expansion anisotropy of the individual grains. It follows, therefore,

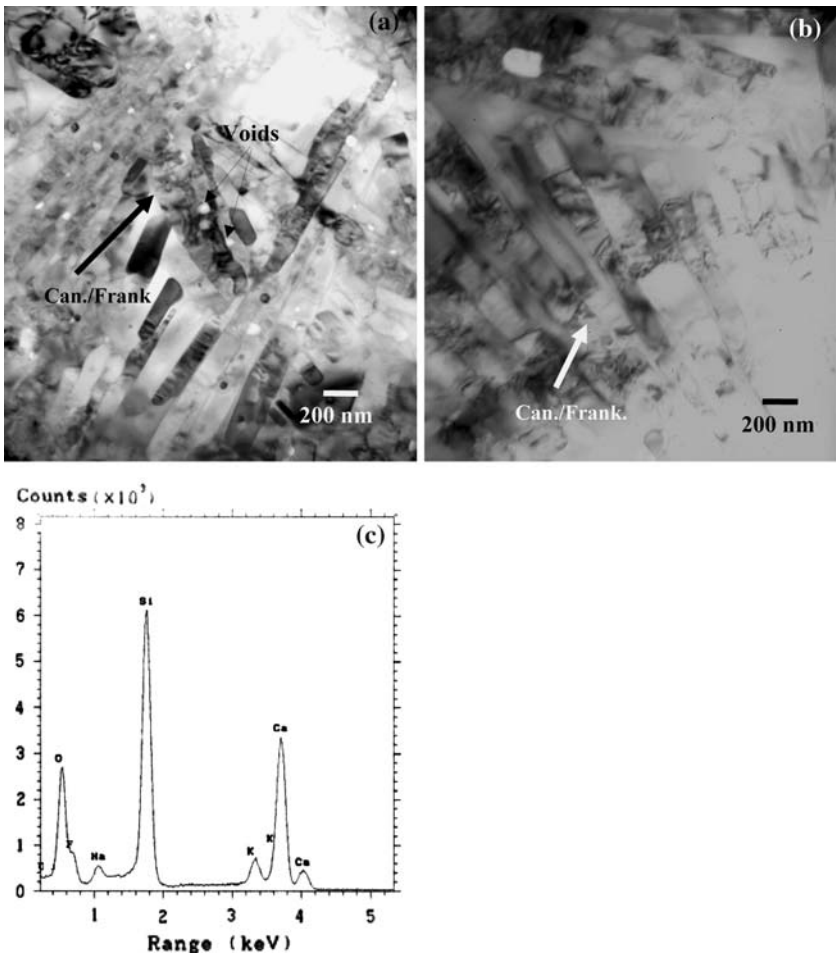

Fig. 2 Bright field (BF) TEM images of (**a**) GCB800, (**b**) GCB900 and (**c**) EDS trace of lath crystal

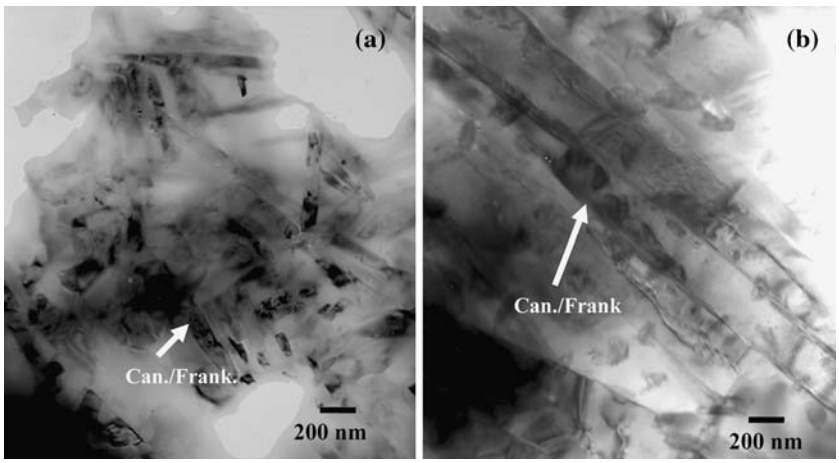

Fig. 3 BF TEM images of GCC800 and GCC900

that the finer the microstructure, the more tortuous the path for fracture, and therefore, the higher the fracture toughness. Consequently, all samples heat-treated at 900 °C, which exhibited a coarser microstructure showed deterioration in IFT with respect to 800 °C.

The highest value of IFT was observed for GCC800 (2.53 ± 0.02 MPa $m^{1/2}$). According to Miller et al. frankamenite and fluorcanasite dominate at this temperature, but xonotlite is also present. It is possible that thermal expansion mismatch between fluorcanasite, frankamenite and xonotlite enhances the fracture toughness.

Glass D has the lowest fracture toughness and is a composite ceramic material composed of chain silicate phases and fluorapatite. Clearly, the formation of a composite has not enhanced the fracture toughness suggesting that crack propagation is made easier by the presence of the

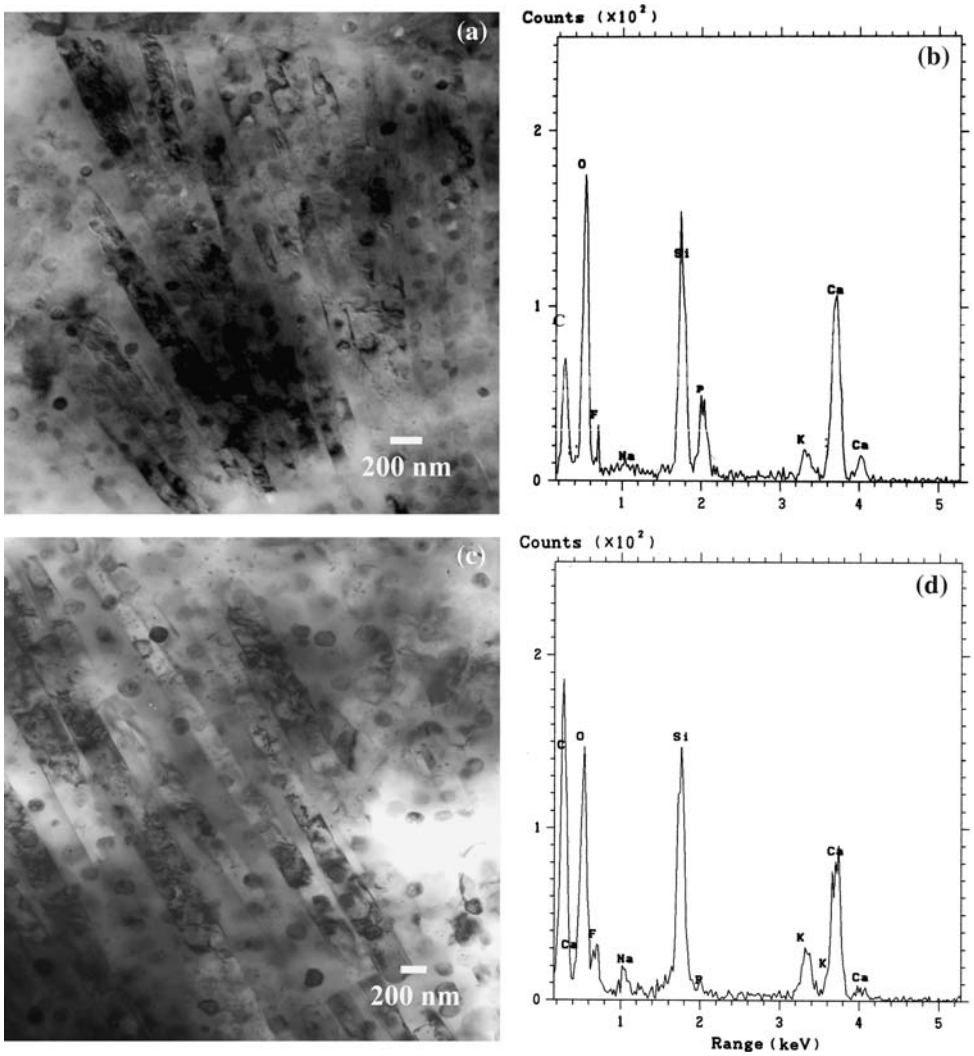

Fig. 4 BF TEM images of (**a**) GCD800, (**b**) EDS trace of spherulite, (**c**) GCD900 and (**d**) EDS trace of lath crystal

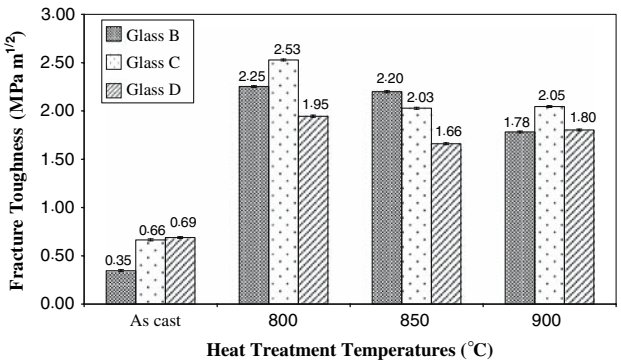

Fig. 5 Vickers indentation fracture toughness of Glass B, Glass C and Glass D, as-cast and heat-treated at 800, 850 and 900 °C

fluorapatite crystals. The microstructure of GCD800 and GCD900 shows that intragranular fluorapatite crystals are distributed throughout the chain silicate laths, Fig. 4a and c. The distribution of the fluorapatite may encourage cracking through the laths rather than along the laths decreasing the extent of crack deflection and thereby lowering IFT.

Comparison with other studies indicates that the IFT values in this work are lower than the fracture toughness values reported by Beall [20] for chain silicate glass-ceramics whose optimum values lay between 4 and 5 MPa $m^{½}$. The compositions studied here have been optimised for biomedical applications, where the response with the human body is paramount [1–3]. Consequently, the small Al_2O_3 content (typically 1.5 wt %) in the original compositions reported by Beall [20] was removed since Al^{3+} ions have been linked with cytotoxicity. Moreover, the values of IFT obtained by indentation are often significantly lower compared to the notched beam methods used by Beall [20].

Biaxial flexural strength

The biaxial flexural strength (BFS) data for Glasses B, C and D, as-cast and heat-treated at 800, 850 and 900 °C are

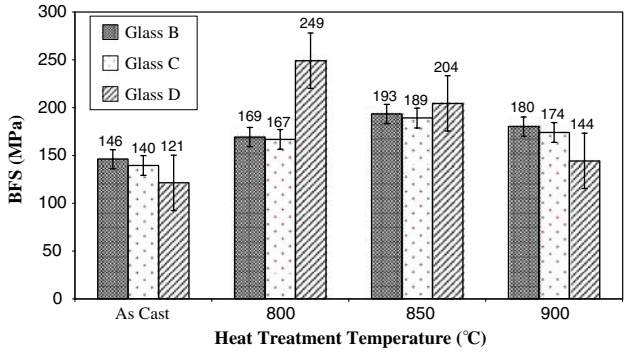

Fig. 6 Biaxial flexural strength of Glass B, Glass C and Glass D, as-cast and heat-treated at 800, 850 and 900 °C

illustrated in Fig. 6. All glasses showed an increase in BFS after ceramming. For Glass B, the BFS is a maximum (193 ± 35 MPa) at 850 °C, which decreased with increasing heat-treatment temperature to 180 ± 27 MPa at 900 °C. In Glass C, BFS rose from 140 ± 48 MPa in the as-cast state to a maximum of 189 ± 10 MPa at 850°C followed by a decrease to 174 ± 31 MPa at 900 °C. In Glass D, a sharp increase in BFS was observed from 121 ± 27 MPa in the as-cast glass to 249 ± 23 MPa at 800 °C followed by a decrease to 204 ± 27 MPa and 144 ± 44 MPa at 850 °C and 900 °C respectively.

The trends in BFS are difficult to explain in terms of microstructure. The finest microstructures are observed at 800 °C and the coarsest at 900 °C. The length of a microcrack or flaw in a ceramic is limited to the grain size, and if the most severe flaw has a half-length equal to the grain diameter, the stress at fracture should be inversely proportional to the square root of the grain size. The flaw sizes should therefore be smallest and the BFS highest at 800 °C, but this is only observed in Glass D. The results may be complicated by uncertainty of the volume fraction and distribution of residual glass, which may vary from composition to composition at the same temperature. However, it is interesting to note that the highest value of BFS occurred in Glass D, which as discussed previously had an intragranular distribution of fluorapatite crystals. The effective average crystallite size is thus reduced in Glass D by the presence of the fluorapatite crystals, and this may explain the higher strength to fracture at 800 °C for this composition.

Conclusions

Stoichiometric fluorcanasite glass-ceramics exhibited poor mechanical properties and crumbled on machining. All modifications resulted in measurable BFS and IFT. IFT was optimised in Glass C (2.53 ± 0.02 MPa $m^{½}$) heat-treated at 800 °C, but this was associated with a low BFS (167 ± 17 MPa). Glass D heat-treated at 800 °C exhibited the highest BFS (249 ± 23 MPa) with reasonable values of IFT (1.95 ± 0.01 MPa $m^{½}$), and was considered the most suitable composition for further research and potential clinical use.

References

1. Jarcho M, Bolen CH, Thomas MB, Bobick J, Kay JF, Doremus RH (1976) Hydroxylapatite synthesis and characterization in dense polycrystalline Form. J Mater Sci 11:2027
2. Hench LL (1998) Bioceramics. J Am Ceram Soc 81:1705
3. Hench LL, Etheridge EC (1982) Biomaterials: an interfacial approach. Academic Press, New York, pp 1–7
4. Kokubo T (1993) A–W glass-ceramic: processing and properties. In: Hench LL, Wilson J (eds) An introduction to bioceramics. World Scientific, London, pp 75–88
5. Beall GH (1991) Chain silicate glass-ceramics. J Non-Cryst Solids 129:163
6. Mirsaneh M, Reaney IM, Hatton PV, James PF (2004) Characterisation of high fgracture toughness k-fluorrichterite fluorapatite glass-ceramics. J Am Ceram Soc 87(2):240
7. da Rocha Barros VM, Salata LA, Sverzut CE, Xavier SP, van Noort R, Johnson A, Hatton PV (2002) *In vivo* bone tissue response to a canasite glass-ceramic. Biomaterials 23:2895
8. Miller CA, Kokubo T, Reaney IM, Hatton PV, James PF (2000) Nucleation and crystallization of canasite-fluorapatite glass ceramics. Int Symp On Crystallization in Glasses & Liquids, Glastech Ber Glass Sci Technol 73(C1):154
9. Miller CA, Reaney IM, James PF, Hatton PV, Kokubo T (2001) Glass ceramics for bone tissue repair. Proc Int Congr Glass 2:601
10. Miller CA, Kokubo T, Reaney IM, Hatton PV, James PF (2002) Formation of apatite layers on modified canasite glass-ceramics in simulated body fluid. J Biomed Mater Res 59:473
11. Miller CA, Reaney IM, Hatton PV, James PF (2004) Crystallization of canasite/frankamenite-based glass-ceramics. Chem Mater 16:5736
12. Bandyopadhyay-Ghosh S, Reaney IM, Hurrell-Gillingham K, Brook IM, Hatton PV (2005) Evaluation of modified flurocanasite glass-ceramics for bone tissue augmentation. Key Eng Mater 284–286:557
13. Bandyopadhyay-Ghosh S, Reaney IM, Brook IM, Hurrell-Gillingham K, Johnson A, Hatton PV (2007) *In vitro* biocompatibility of fluorcanasite glass-ceramics for bone tissue repair. J Biomed Mater Res: Part A 80A(1):175
14. Kanchanarat N, Miller CA, Hatton PV, James PF, Reaney IM (2005) Early stages of crystallization in canasite-based glass ceramics. J Am Ceram Soc 88:3198
15. Ponton CB, Rawlings RD (1989) Vickers indentation fracture toughness test: part 2 application and critical evaluation of standardized indentation toughness equations. Mater Sci Tech 5:961
16. Matsumoto RLK (1987) Evaluation of fracture toughness determination methods as applied to ceria-stabilized tetragonal zirconia polycrystal. J Am Ceram Soc 70(12):C366
17. Morrell R (1998) Biaxial flexural strength testing of ceramic materials. National Physical Laboratory, Teddington, Middlesex, UK
18. Shetty DK, Rosenfield AR, McGuire PA, Bansal GK, Duckworth WH (1980) Biaxial flexure tests for ceramics. Ceram Bull 59:1193
19. Wolcott CC (1994) Canasite apatite glass-ceramics. US Patent 5, 336, 642
20. Beall GH, Chyung K, Stewart RL (1986) Effect of test method and crack size on the fracture toughness of a chain-silicate glass ceramics. J Mater Sci 21:2365